

A Numerical Investigation of CuO-Water Nanofluid in Different Geometries by Two-Phase Euler-Lagrange Method

I. Vasefi and M. Alizadeh

Department of Mechanical Engineering,
Iran University of Science and Technology, Tehran, Iran

Submitted: Sep 23, 2013; **Accepted:** Nov 25, 2013; **Published:** Nov 30, 2013

Abstract: Developing of laminar forced convection flow of a CuO-water nanofluid in different geometries is investigated numerically. The steady state of a three dimensional flow under uniform heat flux boundary condition on the outer wall is considered. Two-phase approach is employed to evaluate the developing laminar forced convection flow. The effect of different forces on particle movement is considered. The velocity and temperature profiles are presented in the fully developed region. The axial development of temperature and convective heat transfer coefficient at the outer wall is shown and discussed. The effects of nanoparticles concentrations on the flow and the convective heat transfer behavior are investigated. The results show significant enhancement of heat transfer of nanofluids. Also, the shape of the duct can have a large effect on heat transfer coefficient.

Key words: Water-CuO nanofluid • Two-phase Euler-Lagrange approach • Different Geometry • Laminar forced convection

INTRODUCTION

Most conventional heat transfer fluids, such as water and Ethylene Glycol have limited capabilities in term of thermal properties that may cause severe restrictions in many thermal applications. While many considerable research and efforts has been deployed, a clear and urgent need does exist to date to develop new tactics in order to improve the effective thermal behaviors of these fluids. Opposite of these fluids, most solids, especially metals, have much higher thermal conductivity. Therefore, it is clear that fluids with suspended solid particles have better heat transfer properties compared to conventional heat transfer fluids. But practical applications show coolants with suspended particles of millimeter or micrometer size have some problems, such as instability of particles, erosion and flow duct clogging and extra pressure drop in the flow duct [1-3]. New developments in producing nanosize metallic or nonmetallic particles have allowed production of a new kind of fluid called nanofluid. The nanofluid is a kind of fluid containing small quantity of nanoparticles that are uniformly and stably suspended

in a liquid. The dispersion of a small amount of solid nanoparticles in conventional fluids changes their thermal conductivity remarkably [4, 5].

Xuan and Li [6] investigated flow and convective heat transfer characteristics of Cu-water nanofluids through a straight tube with a constant wall heat flux boundary condition experimentally. Results showed that nanofluids enhances heat transfer rate compared to pure water considerably. They also claimed that the friction factor for the nanofluids at low volume fraction don't cause extra penalty in the pumping power. Eastman *et al.* [7] reported that the heat transfer coefficient of CuO-water nanofluid containing 0.9% volume CuO was 15% higher than that of pure water. Tofik *et al.* [8] investigated the heat transfer characteristics of Al_2O_3 -water and CuO-water nanofluids in square cross-section duct. Their results indicated that a considerable heat transfer enhancement has been achieved by both nanofluids compared with base fluid. However, CuO-water nanofluid showed better heat transfer augmentation compared with Al_2O_3 -water nanofluid through square cross-section duct. It has been

shown that the effect of particle concentration is more considerable in the turbulent flow regime than the laminar flow [9]. In a comparison between particle sizes it was observed at the same volume fraction, nanofluid with smaller particles show higher heat transfer coefficient than that with larger particles [10]. Mirmasoumi and Behzadmehr [11] have studied the effects of nanoparticle mean diameter on the heat transfer and flow behavior into a horizontal tube under laminar mixed convection condition. Their calculated results demonstrate that the convection heat transfer coefficient significantly increases with decreasing the nanoparticles means diameter.

In this paper, developing of laminar forced convection flow of a CuO-water nanofluid in different geometric cross-section ducts investigated numerically. The effect of the shape of cross-section on heat transfer is shown and discussed. Two-phase approach is employed to evaluate the developing laminar forced convection flow. The effect of fluid forces such as thermophoretic and Brownian forces on particles and their mutual interactions with each other is addressed and studied. The equations are solved by means of control volume method. Comparisons between results are presented for different particle volume fraction. The numerical simulation results are also compared with analytical data of Shah and London [12].

Mathematical Model: In this study, an Euler-Lagrange approach is used to investigate fluid flow and particles motion. In two phase Euler-Lagrange approach, the fluid phase is considered continuous while nanoparticles are dispersed through it. Consequently, conservative equations are considered for the fluid phase while the position of nanoparticles is determined by Newton's second law of motion. In dilute suspensions, particle motion is mainly controlled by fluid forces such as gravity, pressure gradient, thermophoretic and Brownian. Coupling of the continuous fluid phase and the discrete phase is explained by Newton's second law of motion which enters the momentum equation as a source term. Consequently, the conservative equations are written as below:

Continuity equation:

$$\nabla \cdot (\rho_{eff} \mathbf{V}_f) = 0 \quad (1)$$

Momentum equation:

$$\nabla \cdot (\rho_f \mathbf{v}_f \mathbf{v}_f) = \nabla p + \nabla (\mu_f \nabla \mathbf{v}_f) + \mathbf{S}_{p,m} \quad (2)$$

Where $\mathbf{S}_{p,m}$ in Eq. (2) is the source term which represents the momentum transfer between fluid and particles. It can be calculated from momentum variation of the particles as they move through fluid phase of the control volume:

$$\mathbf{S}_{p,m} = \sum m_p \mathbf{F} \Delta t \quad (3)$$

where, m_p is particle mass and \mathbf{F} is the total force per unit particle mass acting on the particle and will be discussed later.

The formal statement for the equation of particles' motion is that the change rate of momentum within the control volume is equal to the forces acting on the particle:

$$\mathbf{F} = \frac{d\mathbf{v}_p}{dt} \quad (4)$$

where, \mathbf{v}_p is the particle velocity and \mathbf{F} is the force per unit of mass. The \mathbf{F} in Eq. (4) is comprised of body forces and various hydrodynamic forces, which includes effects of gravity, drag force, Saffman's lift force, virtual mass force, Brownian force and thermophoretic force.

$$\mathbf{F} = \mathbf{F}_G + \mathbf{F}_D + \mathbf{F}_L + \mathbf{F}_V + \mathbf{F}_T + \mathbf{F}_B \quad (5)$$

where, \mathbf{F}_G is the gravity force and can be calculated by:

$$\mathbf{F}_G = \frac{(\rho_p - \rho_f) \mathbf{g}}{\rho_p} \quad (6)$$

The drag force i.e. \mathbf{F}_D can be obtained from different formulas. For sub-micron particles, a form of Stokes' drag law can be used [13]. In this case, \mathbf{F}_D is defined as:

$$\mathbf{F}_D = \frac{18\mu_f}{d_p^2 \rho_p C_c} (\mathbf{v}_f - \mathbf{v}_p) \quad (7)$$

where, C_c is Cunningham correction factor to Stokes' drag law, which can be obtained from:

$$C_c = 1 + \frac{2\lambda}{d_p} (1.257 + 0.4e^{-(1.1d_p/2\lambda)}) \quad (8)$$

Where, λ is the molecular mean free path.

The Saffman lift force (\mathbf{F}_L) is due to the pressure distribution developed on the particle due to rotation induced by a velocity distribution [14].

$$\mathbf{F}_L = \frac{2K\nu^{1/2}\rho_f d_{ij}}{\rho_p d_p (d_{ij} d_{ij})^{1/4}} (\mathbf{v}_f - \mathbf{v}_p) \quad (9)$$

where, $K = 2.594$ and d_{ij} is tensor of deformation. This form of the lift force is recommended for small particle Reynolds numbers. Also, the particle Reynolds number based on the particle-fluid velocity difference must be smaller than the square root of the particle Reynolds number based on the shear field [15]. Since this restriction is valid just for submicron particles, it is recommended to use the formula only for particles having sizes of below micrometer.

The forces due to acceleration of the relative velocity can be divided into two types; virtual mass force and Basset force. The virtual mass effect is related to the force required to accelerate the surrounding fluid, while the Basset term describes the force due to lagging boundary layer development with changing velocity [15]. In this study, Basset term effect is negligible against virtual mass force and is neglected.

The virtual mass force can be obtained by:

$$\mathbf{F}_V = \frac{\rho_f}{2\rho_p} (\dot{\mathbf{v}}_f - \dot{\mathbf{v}}_p) \quad (10)$$

The thermophoretic force (\mathbf{F}_T) arises due to temperature gradient in the continuous phase. The greater molecular velocities on one side of a particle due to higher temperature increases the momentum exchange and creates a force in the direction of decreasing temperature. The following formula which was first introduced by Talbot [16] is used for the thermophoretic force and yields the best fit with the experimental data over a wide range of Knudsen numbers and thermal conductivity ratios.

$$\mathbf{F}_T = -6\pi\mu_f^2 d_p C_s \frac{1}{\rho_f (1 + 6C_m Kn)} \frac{k_f/k_p + 2C_t Kn}{1 + 2k/k_p + 4C_t Kn} \frac{\nabla T}{m_p T} \quad (11)$$

Where, Kn is Knudsen number and $C_s = 1.17$, $C_m = 2.28$ and $C_t = 4.36$.

If the size of particle suspended in a fluid is very small (less than a micron), its motion will be affected by discrete nature of the molecular motion, exhibiting a

random motion due to collisions between molecules and particle (Brownian motion). For particles smaller than micron, the effects of Brownian motion can be included in the additional force term. Different components of the Brownian force (\mathbf{F}_B) are modeled as a Gaussian white noise process being the spectral intensity of $S_{n,ij}$ given by [17]:

$$S_{n,ij} = S_0 \delta_{ij} \quad (12)$$

where, δ_{ij} is the Kronecker delta function and

$$S_0 = \frac{216\nu k_B T_f}{\pi^2 \rho_f d_p^2 \left(\frac{\rho_p}{\rho_f}\right)^2 C_c} \quad (13)$$

where, T is the absolute temperature of the fluid, ν is the kinematic viscosity and k_B is the Boltzmann constant. Amplitudes of the Brownian force components are of the following form:

$$F_{bi} = \zeta_i \sqrt{\frac{\pi S_0}{\Delta t}} \quad (14)$$

where, ζ_i are zero-mean, unit-variance-independent Gaussian random numbers. The amplitudes of the Brownian force components are individually evaluated during each time step.

Energy equation:

$$\nabla \cdot (\rho_f c_{p,f} \mathbf{v}_f T_f) = \nabla \cdot (k_f \nabla T_f) + S_{p,e} \quad (15)$$

where, $S_{p,e}$ in Eq. (15) is the source term which gives the energy transfer between fluid and particles. It is can be calculated by computing the energy variation of particles as they pass through the fluid phase of control volume, as below:

$$S_{p,e} = \sum \dot{Q} \Delta t \quad (16)$$

where, \dot{Q} is the total efflux due to convective heat transfer acting on the particle and is determined using this equation:

$$\dot{Q} = Nu \pi d_p k_f (T_p - T_f) \quad (17)$$

where, Nu is evaluated using the correlation of Ranz and Marshall [18]:

Table 1: Different geometry cross section

Shape of duct	b/a
	-
	1
	4.0
	-

Table 2: Comparison of theoretical solution of Shah & London with numerical simulation

Shape of duct	$(f \cdot \text{Re}_{D_h})_t$	$(f \cdot \text{Re}_{D_h})_n$	% Error	Nu_t	Nu_n	% Error
Circle	64.00	63.67	0.515	4.36	4.38	-0.458
Rectangle 1:1	56.91	57.06	-0.263	3.61	3.60	0.277
Rectangle 4:1	72.93	72.34	0.808	5.33	5.35	-0.375
Triangle 1:1:1	53.35	53.45	-0.187	3.11	3.10	0.321

$$Nu = 2.0 + 0.6 \text{Re}_d^{1/2} \text{Pr}^{1/3} \quad (18)$$

Having established heat balance around the particle, the convection heat transfer to the fluid must be equal to the variation rate of particle energy.

$$m_p c_{p,p} \frac{dT_p}{dt} = \dot{Q} \quad (19)$$

Boundary Conditions: The geometry is aduct consistdifferent geometry cross-section that all of them contain 1 m length and hydraulic diameter of 8mm. The geometries are shown in Table 1. It is obvious that they may have different width and height. At the tube inlet, profiles of uniform axial velocity and temperature T_0 ($=300\text{K}$) is assumed. At the tube outlet section, the fully developed condition is assumed, that is to say all axial derivatives are zero. No-slip conditions and uniform heat flux are imposed on the duct outer wall. The secondary flow components are also assumed negligible in laminar flow.

Numerical Method and Validation: This set of nonlinear differential equation was discretized with the control volume technique. In flow simulation for the convective and diffusive terms, a second order upwind method was used while the SIMPLE procedure was employed for the velocity-pressure coupling. The grid is non-uniform. It is finer near walls where the velocity and temperature gradients are large. Several different grid distributions have been tested to ensure that the calculated results are grid independent.

In order to demonstrate the validity and precision of the model and numerical procedure, a comparison with analytical solutions for distilled water has been done. Solutions for different geometries have been obtained by Shah and London [12] and compared with numerical solution in Table 2 in terms of a Reynolds number Re_{D_h} based on an equivalent or hydraulic diameter defined as $D_h = 4A/P$, where A is the cross-sectional area and P is the perimeter of the duct. The Nusselt number is also investigated for constant heat transfer rate.

In above table, f represents friction coefficient and subscript t and n denote theoretical solution and numerical solution, respectively. It can be seen that numerical results have a good agreement with theoretical results, while the maximum error for hydrodynamic part is 0.515% and the maximum error for heat transfer part is 0.458%. The results show that the shape of the duct may cause a large alter on heat transfer and pressure drop.

RESULTS AND DISCUSSION

Numerical simulations have been carried out for four different geometry cross sections and wide range of particles volume fraction. The study is done at $\text{Re}=100$ for all geometries. In Figure 1a the effect of nanoparticle volume fraction on convective heat transfer coefficient for a duct with circle cross-section is shown. It is observed that heat transfer enhances with nanoparticle volume fraction.

It can be seen that enhancement increases along the duct's length smoothly and it exceeds 26% at the outlet of duct for $\Phi=3\%$. The study is performed at low Reynolds

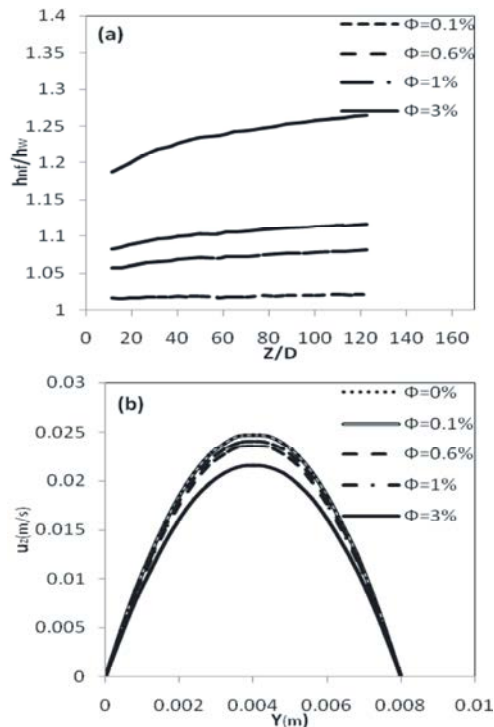


Fig. 1: (a) comparison of nanofluid convective heat transfer in different particle volume fraction. (b) velocity profile at the outlet of duct for $Re=100$ & circle cross-section duct

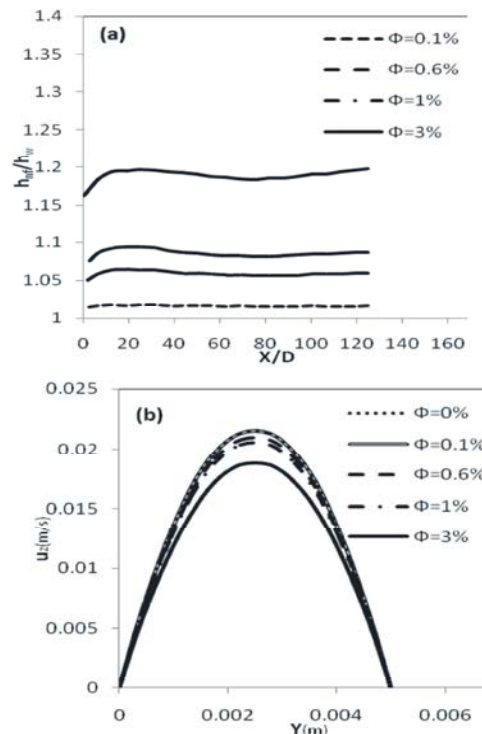


Fig. 3: (a) comparison of nanofluid convective heat transfer in different particle volume fraction. (b) Velocity profile at the outlet of duct for $Re=100$ & rectangle (4:1) cross-section duct

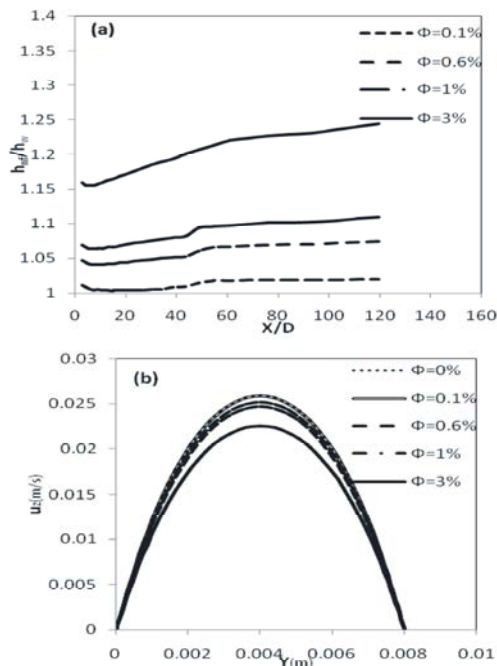


Fig. 2: (a) comparison of nanofluid convective heat transfer in different particle volume fraction. (b) velocity profile at the outlet of duct for $Re=100$ & square cross-section duct

number; therefore the thermal conductivity plays a main role in heat transfer and increases heat transfer rate along duct. In Figure 1b the fully developed velocity profile at the outlet of duct is shown. It is observed that heavy CuO particles change the velocity profile and decrease the maximum of that, while the total mass rate remains constant. In Figure 2a convective heat transfer of CuO-water nanofluid in square duct at $Re=100$ is shown. The enhancement in square looks like circle cross-section entirely, but the rate of enhancement in rectangle is more considerable than circle. For instance, it starts from 15% at the inlet of duct for $\Phi=3\%$ and exceeds 28% at the outlet of duct, while the rate of enhancement in circle duct doesn't change significantly.

Figure 2b shows the velocity profile at the outlet of rectangle duct for $Re=100$. Similar to circle duct, the maximum value of velocity has a reverse relation with nanoparticles volume fraction.

It is also seen that peak of velocity occurs at the middle of duct cross-section, similar to circle duct. Also, the characteristics of velocity profiles didn't change significantly. Figure 3a shows the developing of the convective heat transfer coefficient in rectangle (4:1) duct.

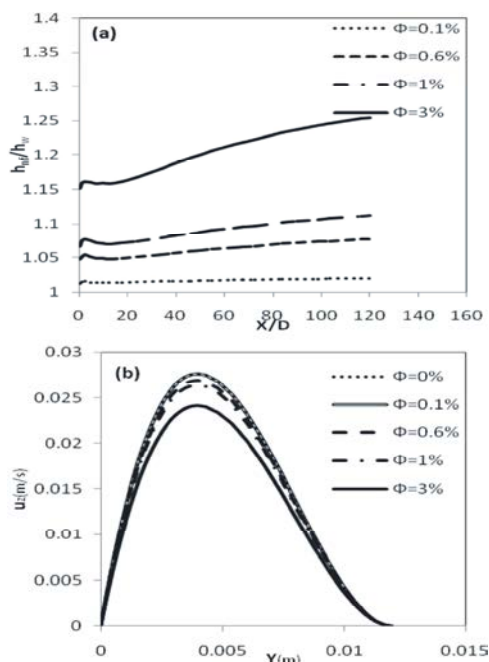


Fig. 4: (a) comparison of nanofluid convective heat transfer in different particle volume fraction. (b) Velocity profile at the outlet of duct for $Re=100$ & triangle (1:1:1) cross-section duct

Like other plots, the convective heat transfer increases with particle volume fraction. But the enhancement in heat transfer is less than square; while the enhancement about 28% observed in square, the enhancement doesn't exceed from 20% in rectangle (4:1). In Figure 3b the developed profiles of velocity for rectangle (4:1) are shown. The profiles have same trends, but the maximum of profiles are reduced considerably in width orientation. In Figure 4a convective heat transfer of CuO-water nanofluid for triangle cross-section duct at $Re=100$ is shown. Similar to square the enhancement in heat transfer increases along duct and exceeds 26% at the outlet of duct.

The fully developed velocity in triangle duct is shown in figure 4b. As expected, the profiles are not parabolic and the maximum of velocity doesn't occur at the middle of height. But like other profiles heavy CuO particles reduce the maximum of velocity but compared with rectangle (4:1), this reduction isn't significant.

CONCLUSIONS

The flow and convective heat transfer characteristics of CuO-water nanofluid in different geometry is investigated by numerical technique. The suspended

nanoparticles remarkably enhance heat transfer process and this enhancement increases with nanofluid volume fraction. The effect of cross-section on nanofluid flow field was investigated and observed that it can alter the rate of heat transfer enhancement and profiles of velocity for different nanoparticles volume fraction.

REFERENCES

1. Kobliski, P., S.R. Phillpot, S.U.S. Choi and J.A. Eastman, 2002. Mechanism of Heat Flow in Suspension of Nano-Sized Particle (Nanofluids), *Int. J. Heat Mass Transfer*, 45: 855-863.
2. Xie, H., J. Wang, T. Xi and Y. Liu, 2002. Thermal Conductivity of Suspensions Containing SiC particles, *Int. J. Thermophys.*, 23: 571-580.
3. Wang, B.X., L.P. Zhou and X. F. Peng, 2003. A Fractal Model for Predicting the Effective Thermal Conductivity of Fluid with Suspension of Nanoparticles, *Int. J. Heat Mass Transfer*, 46: 2665-2672.
4. Heris, S.Z., S.G. Etemad and M.N. Esfahany, 2006. Experimental investigation of oxide nanofluids laminar flow convective heat transfer, *International Communications Heat Fluid Flow*, 33: 529-535.
5. Heris, S.Z., M.N. Esfahany and S.G. Etemad, 2007. Experimental investigation of convective heat transfer of CuO/water nanofluid in circular tube, *International Journal of Heat Fluid Flow*, 28(2): 203-210.
6. Xuan, Y. and Q. Li, 2003. Investigation on convective heat transfer and flow features of nanofluids, *Journal of Heat Transfer*, 125: 151-155.
7. Eastman, J.A., S.U.S. Choi, G. Soye, L.J. Thompson and R.J.D. Melfi, 1999. Novel Thermal Properties of Nanostructured Materials, *Mater. Sci. Forum*, 312-314: 629-634.
8. Taofik H. Nassan, S. Zeinali Heris and S.H. Noie, 2010. A comparison of experimental heat transfer characteristics for Al_2O_3 /water and CuO/water nanofluids in square cross-section duct, *International Communications in Heat and Mass Transfer*, 37: 924-928.
9. He, Y., Y. Jin, H. Chen, Y. Ding, D. Cang and H. Lu, 2007. Heat transfer and flow behaviour of aqueous suspensions of TiO_2 nanoparticles (nanofluids) flowing upward through a vertical pipe, *International Journal of Heat and Mass Transfer*, 50: 2272-2281.

10. Anoop, K.B., T. Sundararajan and S.K. Das, 2009. Effect of particle size on the convective heat transfer in nanofluid in the developing region, *International Journal of Heat and Mass Transfer*, 52: 735-743.
11. Mirmasoumi, S. and A. Behzadmehr, 2008. Effect of nanoparticles mean diameter on mixed convection heat transfer of a nanofluid in horizontal tube, *Int. J. Heat Fluid Flow*, 29: 557-566.
12. Shah, R.K. and A.L. London, 1978. *Laminar Flow Forced Convection in Ducts*, Academic Press, New York, NY.
13. Ounis, H., G. Ahmadi and J.B. McLaughlin, 1991. Brownian diffusion of sub micrometer particles in the viscous sub layer, *J. Colloid Interface Science*, 143(1): 266-277.
14. Saffman, P.G., 1965. The lift on a small sphere in a slow shear flow, *J. Fluid Mechanics*, 22: 385-400.
15. Crowe, C., M. Sommerfeld and Y. Tsuji, 1997. *Multiphase flows with droplets and particles*, CRC Press, ISBN: 0-8493-9469-4.
16. Talbot, L., 1980. Thermophoresis of particles in a heated boundary layer, *J. Fluid Mechanics*, 101(4): 737-758.
17. Li, A. and G. Ahmadi, 1992. Dispersion and deposition of spherical particles from point sources in a turbulent channel flow, *Aerosol Science and Technology*, 16: 209-226.
18. Ranz, W.E. and W.R. Marshall, 1952. Evaporation from Drops, Part I. *Chemical Engineering Program*, 48(3): 141-146.